JTTEE5 4:133-136

"Smart" Coatings: A Technical Note

M. Fasching, F.B. Prinz, and L.E. Weiss

The integration of sensors into thermally sprayed coatings can provide feedback about the functional status and operating history of the coatings as well as of the coated structures and surrounding environments. Sensors can be spray-formed directly on coatings using masking techniques. Production of coatings that contain embedded sensors opens up a new dimension for thermal spray technology: "smart" coatings. This paper describes the results of initial experiments to spray-form thermocouples, humidity sensors, strain gages, and sensor arrays.

1. Introduction

EVER SINCE Schoop (Ref 1) first conceived of thermal sprayed coatings in 1917, the range of available coating materials has increased, the quality of the coatings has improved, and hundreds of new coating applications have evolved. Thermal spraying has been used to produce both near-net and net shapes (Ref 2, 3), but its primary use has been in coating applications. This paper describes how coating and shaping methodologies can be combined to produce novel coatings that contain embedded sprayed sensors. The integration of sensors, such as thermocouples and strain gages, into a coating (Fig. 1) could provide feedback about the functional status and operating history of the coating as well as of the coated structure and surrounding environment. Production of coatings with embedded sensors opens up a new dimension for thermal spray technology: "smart" coatings.

Sprayed materials can be selectively deposited or shaped using masking techniques (Ref 3). Discrete shapes, such as sensors, can therefore be formed with appropriately shaped masks. For example, a temperature sensor can be constructed by forming a thermocouple junction between two dissimilar metals (Fig. 2). A mask of the first metal shape, or "thermoleg," is placed on an insulating coating (or on a nonconducting substrate), and metal is sprayed over it. The mask is then removed, leaving a thin wire trace connected to a small pad that will form the junction. The second thermoleg is similarly deposited using another mask aligned on the substrate so that only the pad of the first thermoleg is exposed to the second material. Additional coatings can be sprayed onto the sensor to fully embed it.

Several sprayed sensors have been manufactured to investigate the feasibility of smart coating technology. This paper presents the results of these initial experiments. The first section describes the production and evaluation of sprayed thermocouples. Novel configurations are described, including multisensor arrays and a multilayer humidity sensor. These sensors have not been tested under operational conditions; however, the results encourage further development of this technology.

Keywords: manufacturing, sensors, sprayed thermocouples, strain gages

M. Fasching, The Department of Electrical Engineering, Technical University of Vienna, Austria; **B. Prinz** and **L.E. Weiss,** The Robotics Institute and Engineering Design Research Center, Carnegie Mellon University, Pittsburgh, PA 15213-3890, USA

2. Sprayed Thermocouples

Thermocouples were fabricated using the mask-and-spray method outlined in Section 1. The goal was to characterize sprayed thermocouples and to determine the effects of spray parameters on the thermocouple voltages. Spraying was performed using a two-wire electric arc torch with air atomization. Masks were constructed of conventional adhesive paper cut to shape with a CO_2 laser (Ref 4). The resulting thermocouple junctions were 2.5 mm across, and the traces leading to the junctions were 1.5 mm wide and 13 cm long. Feature sizes achievable with this approach are on the order of 200 μm. Smaller feature sizes have been produced using other masking materials and spray apparatus (Ref 5).

The substrates were flat, sandblasted (SAE 40 grit at 80 psi, with a 20 cm standoff) porcelain tiles with thinly (0.5 to 3.0 μm) sprayed iron coatings that were oxidized at 1000 °C for 20 min. The iron coatings were required as an intermediate layer to ensure good adhesion of the thermocouples to the substrates. Sprayed copper, which was one of the materials used to make the thermocouples, peeled away when sprayed directly onto the

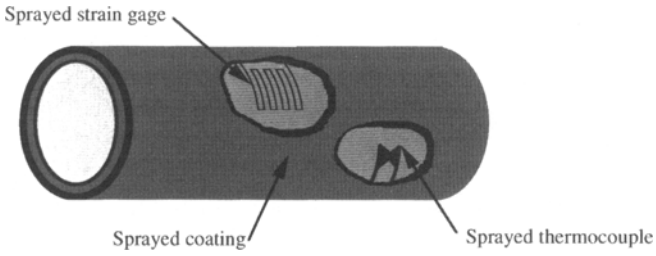

Fig. 1 "Smart" coating with embedded sensors

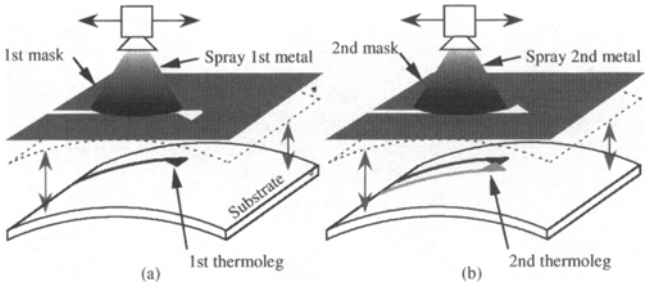

Fig. 2 Sprayed thermocouple fabrication

tiles. The process of oxidizing the iron to make it an insulator also reduced internal stresses and further improved adhesion.

Although conventional thermocouples are fabricated with standard thermocouple wires, the material compositions of these wires were not available in feedstock suitable for arc spray apparatus. Instead, the compositions listed in Table 1 were used. These materials can be combined to produce three types of thermocouples analogous to the standardized T, J, and E types (see Table 2). For example, the sprayed junction of a Cu-CuNi thermocouple is shown in Fig. 3.

One hundred and forty sensors were fabricated with a range of spray parameters (Table 3). Each thermocouple was tested from 25 to 200 °C, and an average thermocouple voltage per degrees Kelvin was calculated. Figure 4 shows a block diagram of the measurement system that was used to test the thermocouples. A Peltier element, which is capable of both cooling and heating, was used to maintain a constant temperature at the measurement connections. The junction of the thermocouple was heated with a resistor. The thermocouple voltages and temperatures were recorded on a 80535-based microprocessor and then transferred to a personal computer for statistical analysis. The measurement accuracy of the system was ±0.25 °C.

Table 2 summarizes the experimental results of the measurements from the sprayed thermocouples. These data suggest that the functional characteristics of these sensors are reproducible with a small deviation from their mean values. These results compare favorably with conventional thermocouples, which are manufactured with tolerances of ±4% in the temperature range of 20 to 200 °C. In addition, the spray production process is robust in that the thermocouple voltage is not strongly dependent on the spray conditions (including arc voltage, wire speed, gas flow rate, and torch standoff). Because thermocouples are very sensitive to oxidation, a reduced standard deviation could be expected if inert gases were used for spraying.

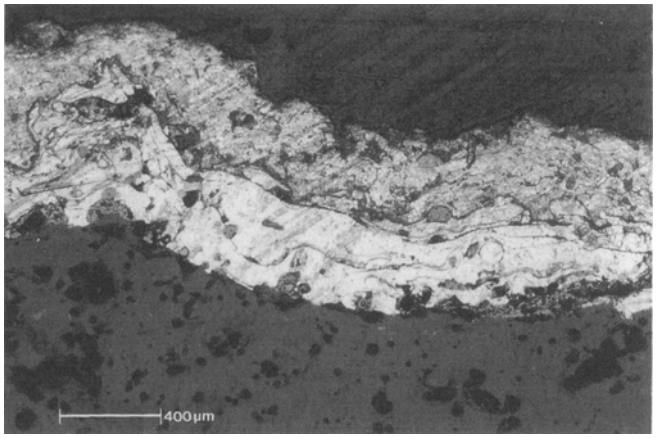

Fig. 3 Sprayed junction of a Cu-CuNi thermocouple

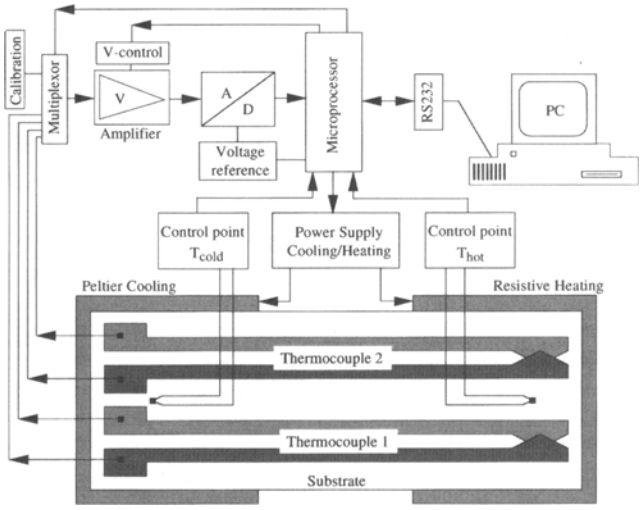

Fig. 4 Block diagram of the test equipment

Table 1 Thermocouple material combinations

Sprayed material	Substituted for thermocouple wire
67Cu-31Ni	60Cu-40Ni
80Ni-20Cr	90Ni-10Cr
1080 steel	Iron

Table 2 Thermocouple voltage per degree Kelvin (μV/K) at 20 °C

Type	Material	No. of thermocouples manufactured	Mean	Standard deviation	Minimum	Maximum	Standard thermocouple mean
T	Cu-CuNi	52	37.93	0.6	36.96	39.00	38.0
E	NiCr-CuNi	46	45.57	1.92	40.77	47.66	56.0
J	Fe-CuNi	26	44.55	0.76	43.48	46.10	52.6

Table 3 Range of arc spray parameters

Material	Wire diameter, mm	Voltage, V	Wire speed, cm/min	Standoff distance, cm	Current, A
Cu	1.588	25-35	408-711	12.7-21.59	100-275
Fe	1.588	28-30	284-533	16.51-21.59	170-275
Cu-Ni	0.813	25-35	284-889	12.7-26.67	30-120
NiCr	0.813	25-33	284-889	24.13-26.67	70-120

3. Novel Sensors

Novel sensor configurations can be made easily and quickly with the mask-and-spray approach. For example, Fig. 5 depicts

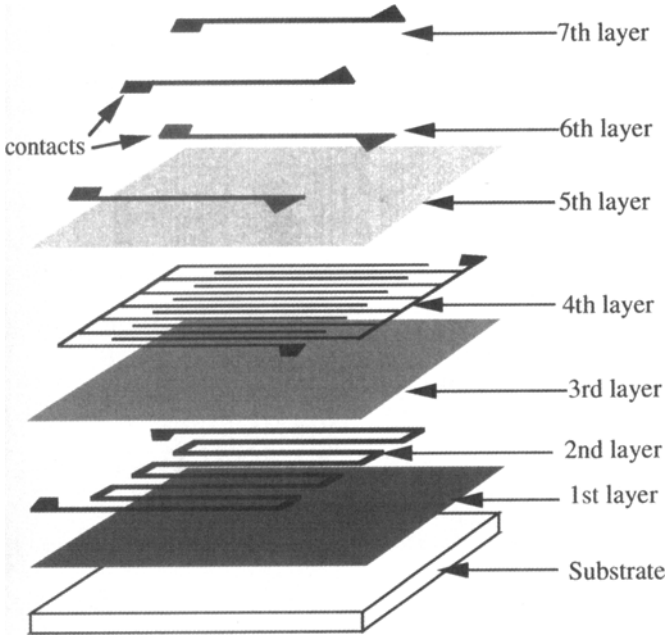

Fig. 5 Humidity sensor layout

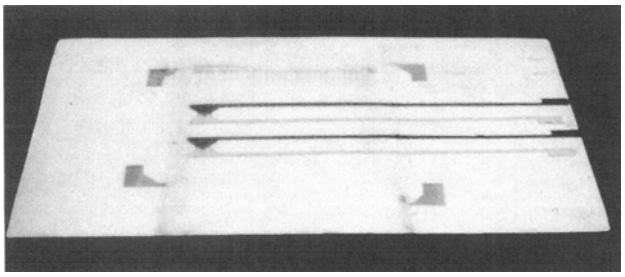

Fig. 6 Humidity sensor fabricated on a 10 by 15 cm steel plate

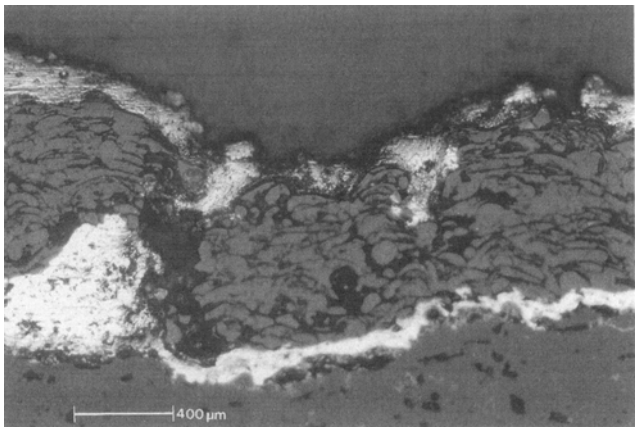

Fig. 7 Penetration of metal into porous Al_2O_3 layer

a multilayered, temperature-controlled humidity sensor that also includes sprayed heating elements. The device, which is shown in Fig. 6, consists of seven sprayed layers:

1. An Al_2O_3 layer (~750 μm thick) that insulates the sensor from the steel substrate
2. A zinc heating element (~50 μm thick, with ~1.5 mm trace widths)
3. A *dense* Al_2O_3 insulating layer (~50 μm thick)
4. A zinc comblike structure (~50 μm thick, with ~1 mm trace widths), aligned above the heater, that serves as the humidity sensor
5. A *porous* Al_2O_3 layer (~500 μm thick) that absorbs moisture and serves as an insulator to the next layer
6. First two thermolegs of two thermocouples (~50 μm thick)
7. Second thermolegs to complete the thermocouples (~50 μm thick)

A flame torch was used to deposit the ceramic insulating layers, although plasma spraying, if available, is preferable. The densities of the Al_2O_3 layers were controlled by varying the torch standoff distances; a small standoff produces a dense insulating layer, whereas a large standoff produces a more porous coating (Ref 6). The amount of porosity was assessed qualitatively. During operation, the porous Al_2O_3 layer (the fifth layer) is kept at constant temperature using feedback from thermocouples to control the current in the heating element (the second layer). Penetrating humidity decreases the impedance of the comblike structure (the fourth layer), which can be measured with an ohm meter.

One difficulty encountered in spraying this device was partial short circuits between layers. Insulating layers with high porosity can be penetrated by sprayed metal particles of subsequent layers. A cross section of the penetration of copper particles into a porous Al_2O_3 layer is shown in Fig. 7. To solve this problem, the porous fifth layer was sprayed to a thickness of 500 μm.

Although the performance specifications of this device have not yet been evaluated, its functionality has been verified. For example, placing the palm of one's hand above the sensor (at a distance of approximately 2.0 to 5.0 cm) changes the resistance from 1 to 30 MΩ due to moisture present in the palm. When the hand is removed, the resistance slowly increases if the heater is not used. If the heater is connected, the resistance change responds more rapidly.

Arrays of sensors are also simple to produce with masking. Rather than gluing discrete sensors in place, multiple sensor patterns can be cut into a single mask to produce an array. For example, a section of a complex temperature-sensing array, with 38 thermocouples and interconnecting wiring, is shown in Fig. 8. The width of the traces on this device are 2.0 mm and the junctions are 3.0 mm across.

4. Discussion

In addition to the devices described to this point, other types of sprayed sensors can also be produced, including strain gages, antennas, and pressure-sensitive switches. Zinc strain gages

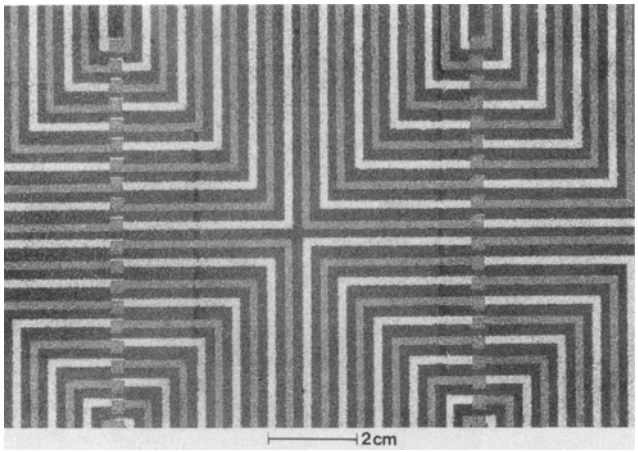

Fig. 8 Sprayed temperature sensor array

have been manufactured, but exhibited poor performance due to the poor mechanical properties of air-atomized, arc-sprayed zinc. Although the electrical resistance of the gages changed in response to an applied strain, they remained deformed once the stress was removed; this was caused by excessive oxidation and poor cohesive bonding of the sprayed zinc. Better spray conditions (e.g., plasma spray and inert atomization), other materials, and/or postprocessing will be required to produce gages (and other sensors) with suitable material properties.

Sprayed sensors have several properties that are not easily achievable with conventional discrete sensors. The use of flexible masking materials allows sprayed sensors to conform to surfaces of complex shape, producing optimal surface contact. The shape of the sensors, as well as its wiring and interconnections, can be individually designed for a particular application. The production and the installation of the sensor and coating occur concurrently, allowing straightforward production of sensor arrays. The sensor can be sealed against the environment by additional coatings. Another advantage is the assortment of new materials that could be applied in sensor manufacturing by using multicomponent powders (Ref 7). Such sensors could be sprayed in a production manufacturing environment. In practice, smart coatings could be produced on the shop floor.

References

1. H. Gunther and M.U. Schoop, *Das Schoopsche Metallspritz*, Franckh, Stuttgart, 1917
2. H. Herman and S. Sampath, Plasma Spray Forming Metals, Intermetallics, and Composites, *JOM*, Vol 45 (No. 7), July 1993, p 42-49
3. L.E. Weiss, F.B. Prinz, D. Adams, and D.P. Siewiorek, Thermal Spray Shape Deposition, *J. Therm. Spray Technol.*, Vol 1 (No. 3), 1992, p 231-237
4. R. Merz, L.E. Weiss, and F.B. Prinz, "Planning Mask Cutting for Thermal Spray Shape Deposition," EDRC 24-74-91, Carnegie Mellon University, Pittsburgh, 1991
5. "DC Arc-Plasma: The Future in the P/M Industry," APS-Materials, Dayton, OH, p 5
6. J.R. Finke and W. Swank, Air Plasma Spraying of Zirconia: Spray Characteristics and Standoff Distance Effect on Deposition Efficiency and Porosity, *Thermal Spray: International Advances in Coatings Technology*, C.C. Berndt, Ed., ASM International, 1992, p 513-518
7. E. Lugscheider, M. Loch, and H.G. Suk, Powder Technology—State of the Art, *Thermal Spray: International Advances in Coatings Technology*, C.C. Berndt, Ed., ASM International, 1992, p 555-559